$HOSO_2-H_2O$ Radical Complex and Its Possible Effects on the Production of Sulfuric Acid in the Atmosphere

Eric T. Aaltonen and Joseph S. Francisco*

Department of Chemistry and Department of Earth and Atmospheric Sciences, Purdue University, West Lafayette, Indiana 47907-1393

Received: August 29, 2002; In Final Form: November 19, 2002

The optimized structure, rotational constants, vibrational frequencies, changes in spin density, and binding energy are calculated for $HOSO_2-H_2O$ using ab initio molecular methods. Structurally, the OH bond of $HOSO_2$ increases in length upon formation of the complex, and the SO bond shortens. The OH stretching frequency of $HOSO_2$ is red-shifted 561 cm^{-1} from its isolated monomer, and the intensity is increased 10-fold. The initial spin density of the separate monomers is rearranged into a ring pattern surrounding the ring structure of the complex. The complex is bound by 10.6 kcal mol^{-1}.

I. Introduction

Numerous studies have been conducted on the conversion of anthropogenic emission of SO_2 to H_2SO_4, a key culprit in global acid deposition.[1,2] The conversion mechanism is widely believed to take place by a series of three reactions as follows:[2−5]

$$SO_2 + OH + M \rightarrow HOSO_2 + M \quad (1)$$

$$HOSO_2 + O_2 \rightarrow SO_3 + HO_2 \quad (2)$$

$$SO_3 + H_2O + M \rightarrow H_2SO_4 + M \quad (3)$$

The first reaction of SO_2 with OH radical catalyzed by a collision partner M has been studied, both theoretically and experimentally.[6−11] The product of reaction 1, the $HOSO_2$ radical, has been studied theoretically[12] and experimentally.[8,13,14] The existence of $HOSO_2$ radical has been confirmed experimentally by Egsgaard et al.[8] with neutralization/reionization mass spectrometry, and vibrational frequencies have been measured by Hashmoto et al.[14] in a low-temperature matrix. An ab initio study of reaction 2, including its reaction complexes and transition states, has been performed.[15] Reaction 2 relies on the extraction of H from $HOSO_2$ to produce SO_3,[15,16] which is essential for reaction 3. The SO_3 reaction with water in the presence of M has been studied extensively.[17−25] This reaction takes place in two distinct steps, as shown here:

$$SO_3 + H_2O + M \rightarrow SO_3-H_2O \quad (4)$$

$$SO_3-H_2O \rightarrow H_2SO_4 \quad (5)$$

An intermediate water complex, SO_3-H_2O, is initially produced and is then converted to H_2SO_4. This two step reaction has an activation barrier of 32.2 kcal mol^{-1}.[22] Additional water present in reaction 4 has been shown to have a catalytic effect, which relies on the formation of another intermediate water complex, SO_3-2H_2O, enroute to a final product of sulfuric acid complexed with water, $H_2SO_4-H_2O$.[22,25] Morokuma and Muguruma[25] proposed and studied three different routes in which an extra water could catalyze the SO_3 conversion:

$$SO_3 + (H_2O)_2 \rightarrow H_2SO_4-H_2O \quad (6)$$

$$SO_3-H_2O + H_2O \rightarrow H_2SO_4-H_2O \quad (7)$$

$$SO_3-2H_2O \rightarrow H_2SO_4-H_2O \quad (8)$$

The activation barriers for these reactions are 0.7 (eq 6), 5.3 (eq 7), and 13 kcal mol^{-1} (eq 8).[25] The second water drastically reduces the activation barrier for the conversion of SO_3. Hofmann-Sievert and Castleman,[26] along with Akhmatskaya et al.,[27] have since shown that the presence of large water clusters such as $(H_2O)_{10}$ further lowers the activation energy, easily allowing the conversion of SO_3 to H_2SO_4. Akhmatskaya[27] has also distinguished the large complex, $[SO_3(H_2O)_2](H_2O)_{10}$, which lowers the activation barrier of reaction 8 by 10 kcal mol^{-1}. In this paper, the possibility of the existence of a water complex in reaction 2 is studied. This complex, $HOSO_2-H_2O$, differs from the SO_3-H_2O and SO_2-H_2O complexes of previous work[22,25−28] because $HOSO_2-H_2O$ is a water complexed with an open shell radical, whereas SO_3 and SO_2 are both closed shell species. Other radical−water complexes such as HO_2-H_2O[29] and $HOCO-H_2O$[30] have been examined previously, and this paper is a similar investigation of the $HOSO_2-H_2O$ complex and possible implications for the mechanism of H_2SO_4 in the atmosphere.

II. Computational Methods

All calculations were performed with GAUSSIAN 98 software.[31] Two levels of theory were used to analyze the $HOSO_2-H_2O$ complex, unrestricted Møller−Plesset theory (MP2)[32,33] and Becke's nonlocal three parameter exchange and correlation functional with the Lee−Yang−Parr correlation functional method (B3LYP).[34,35] In the MP2 calculations, the core orbitals were unfrozen. The four basis sets used for calculations ranged from medium to large in size and were used in conjunction with both MP2 and B3LYP. The sets were 6-311G(d), 6-311++G(2d,2p), 6-311++G(2df,2p), and 6-311++G(3df,3pd).[36,37] The optimized structures of $HOSO_2-H_2O$ calculated with these basis

10.1021/jp021977o CCC: $25.00
Published on Web 02/04/2003

TABLE 1: Optimized Geometries for $HOSO_2$ and $HOSO_2-H_2O$[a]

	$HOSO_2$							
	B3LYP				MP2			
coordinates	6-31G(d)	6-311++ G(2d,2p)	6-311++ G(2df,2p)	6-311++ G(3df,3pd)	6-31G(d)	6-311++ G(2d,2p)	6-311++ G(2df,2p)	6-311++ G(3df,3pd)
R(SO)	1.67	1.65	1.64	1.63	1.65	1.64	1.62	1.61
R(SO′)	1.48	1.46	1.46	1.45	1.47	1.45	1.45	1.44
R(SO″)	1.47	1.45	1.45	1.44	1.46	1.44	1.44	1.43
R(OH)	0.98	0.97	0.97	0.97	0.98	0.97	0.97	0.97
OSO′	107.1	107.9	108.0	108.2	107.4	108.1	108.3	108.5
OSO″	105.2	105.3	105.4	105.5	105.8	105.8	106.0	105.9
HOS	106.9	107.4	108.1	108.5	107.2	106.5	107.0	107.5
O′SOH	23.6	27.8	28.3	28.1	23.5	25.4	26.2	26.8
O″SOH	155.9	160.8	161.0	161.4	158.6	160.7	161.2	162.3
	$HOSO_2-H_2O$							
	B3LYP				MP2			
coordinates	6-31G(d)	6-311++ G(2d,2p)	6-311++ G(2df,2p)	6-311++ G(3df,3pd)	6-31G(d)	6-311++ G(2d,2p)	6-311++ G(2df,2p)	6-311++ G(3df,3pd)
R(SO)	1.63	1.62	1.61	1.60	1.62	1.60	1.59	1.58
R(SO′)	1.49	1.47	1.47	1.46	1.48	1.46	1.46	1.45
R(SO″)	1.47	1.45	1.45	1.44	1.46	1.45	1.44	1.43
R(OH)	1.01	1.00	1.00	1.00	1.01	0.99	1.00	1.00
R(O‴H′)	0.98	0.97	0.97	0.97	0.98	0.96	0.96	0.96
R(O‴H″)	0.97	0.96	0.96	0.96	0.97	0.96	0.96	0.96
R(O‴H)	1.66	1.70	1.69	1.68	1.69	1.69	1.67	1.65
R(O′H′)	2.10	2.29	2.31	2.29	2.19	2.21	2.24	2.23
OSO′	107.9	108.5	108.5	108.7	108.2	108.7	108.8	109.0
OSO″	107.5	107.1	107.3	107.5	107.8	107.7	107.9	108.0
HOS	108.0	107.9	108.4	108.8	108.1	107.0	107.3	107.6
O‴HO	165.1	166.6	166.5	166.3	165.4	166.9	166.7	166.8
HO‴H′	94.0	98.5	99.2	98.3	96.4	97.9	98.4	98.3
HO‴H″	114.2	123.2	124.8	123.8	117.7	124.3	125.2	125.1
O‴H′O′	130.5	123.0	121.9	122.9	126.1	123.7	123.0	123.0
H′O′S	111.0	109.9	110.0	109.8	111.2	110.2	110.3	109.8
O′SOH	17.8	24.1	23.8	23.2	21.5	23.3	23.2	23.3
O″SOH	149.7	157.0	156.5	156.4	156.4	158.4	158.0	158.6
SOHO‴	−22.6	−32.1	−31.4	−31.9	−23.4	−32.7	−32.0	−31.8
H′O‴HO	6.2	18.9	18.5	19.5	4.9	21.3	20.7	20.4
H″O‴HO	114.7	135.4	136.8	136.2	116.1	137.0	137.4	137.0

[a] Bond distances are reported in angstroms. Angles and dihedrals are reported in degrees.

sets were free from any geometrical constraints, resulting in global minima on the energy surface. Because spin contamination may produce inaccurate total energies when performing unrestricted calculations, the total spin value $\langle S^2 \rangle$ was closely monitored. The largest preannihilation deviation from the expected $\langle S^2 \rangle$ value of 0.75 was less then 4%; therefore, spin contamination was considered negligible. Boys−Bernardi counterpoise correction[38] was used to account for basis set superposition error (BSSE), which was negligible (<0.8 kcal mol^{-1}) for the larger basis sets.

III. Results and Discussion

McKee and Li have carried out structural analysis of the $HOSO_2$ radical.[28] They examined the possible geometries of the radical under the C_s and C_1 point groups. Their work showed that within the C_s point group, there is the possibility of trans/cis geometries and two energy states, $^2A'$ and $^2A''$, the second state formed by the promotion of an electron to a σ^* orbital. The lowest energy structure is *cis*-$HOSO_2(^2A')$. However, it is observed that the C_1 structure of $HOSO_2$ is even lower in energy than the *cis*-$C_s(^2A')$. The C_1 geometry is found to be the location of global energy minima across the potential energy surface.[28] The optimized structure of $HOSO_2$ has C_1 geometry with a single oxygen out-of-plane from the other four atoms (see Figure 1). Calculations of the $HOSO_2$ geometries in this paper also produced a C_1 structure, with an HOSO′ dihedral angle of 28.1° (26.8°) at the B3LYP[MP2]/6-311++G(3df,3pd) level. Geometry optimization was done at both the MP2 and the B3LYP level of theory using basis sets ranging from 6-31G(d) to 6-311++G(3df,3pd) in size, and the results of the two different theories are in good agreement with each other and with previous work.[15,28] Optimized bond distances and angles are shown in Table 1. When $HOSO_2$ forms a complex with H_2O, the radical retains C_1 geometry (HOSO′ becomes 23.2° (23.3°)). This geometry retention is beneficial for the stability of the complex since the radical is not being twisted or distorted a significant amount from its original optimized geometry. Figure 2 shows the most stable configuration of $HOSO_2-H_2O$. Numerous structures containing single or double hydrogen-bonded interactions were examined in search of local minima, but each complex yielded the given six-membered ring upon optimization, indicating only a single global minimum. To form the

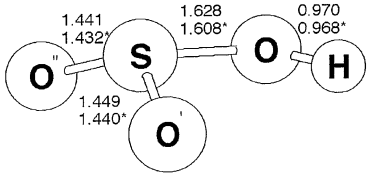

Figure 1. Geometric structure for $HOSO_2$. Numbers without asterisks are from the B3LYP/6-311++G(3df,3pd) while numbers with asterisks are from the MP2/6-311++G(3df,3pd) level of theory.

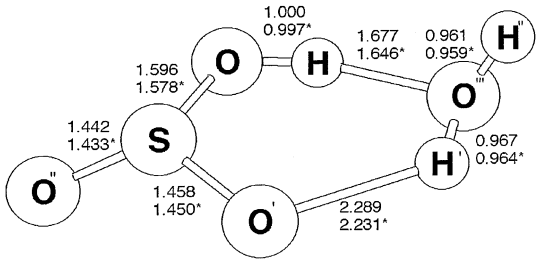

Figure 2. Geometric structure for $HOSO_2-H_2O$. Numbers without asterisks are from the B3LYP/6-311++G(3df,3pd) while numbers with asterisks are from the MP2/6-311++G(3df,3pd) level of theory.

TABLE 2: Rotational Constants[a]

compd	level of theory	basis set	rotational constants A	B	C
		6-31G(d)	8915	8609	4686
	B3LYP	6-311++G(2d,2p)	9052	8874	4778
		6-311++G(2df,2p)	9127	8942	4819
		6-311++G(3df,3pd)	9223	9032	4860
$HOSO_2$		6-31G(d)	9099	8659	4708
		6-311++G(2d,2p)	9213	8908	4799
	MP2	6-311++G(2df,2p)	9349	9018	4866
		6-311++G(3df,3pd)	9442	9105	4907
		6-31G(d)	8605	2402	1961
	B3LYP	6-311++G(2d,2p)	8901	2343	1916
		6-311++G(2df,2p)	8973	2346	1922
		6-311++G(3df,3pd)	9063	3466	1938
$HOSO_2-H_2O$		6-31G(d)	8872	2363	1928
		6-311++G(2d,2p)	9044	2378	1939
	MP2	6-311++G(2df,2p)	9171	2399	1959
		6-311++G(3df,3pd)	9264	2426	1979

[a] Rotational constants reported in MHz.

complex, partial hydrogen bonding occurs between the hydrogen of $HOSO_2$ and the H_2O oxygen and also between one of lone $HOSO_2$ oxygens and one of the hydrogens of H_2O. These two partially bound sites form a six-membered ring with an oxygen and hydrogen para to each other. Distortion of $HOSO_2$ does occur at two sites, and MP2 and B3LYP calculations with the 6-311++G(3df,3pd) basis sets indicate that the length of the OH bond of $HOSO_2$ increased by 3% and the SO bond length decreased by 1% with complex formation. Accordingly, the OH bond is predicted to be weaker in the complex while the SO bond becomes stronger.

Table 2 reports the rotational constants of the isolated monomers and the optimized complex at several levels of theory. From the rotational constants, it can be determined that $HOSO_2$ behaves spectroscopically as a prolate symmetric rotor since $A \approx B > C$. The optimized structure and rotational constants of the complex clearly show that any symmetric nature of the $HOSO_2$ monomer is lost and $HOSO_2-H_2O$ is an asymmetric rotor. The complex should be active in the microwave region of the energy spectrum due to its permanent dipole moment.

The harmonic vibrational frequencies for $HOSO_2$, H_2O, and their resulting radical complex are given in Table 3, and frequencies were calculated using MP2 and B3LYP theories with the 6-311G(d) and 6-311++G(2df,2p) basis sets. The frequency shifts shown in parentheses are calculated by subtracting the vibrational frequencies of the radical complex from the vibrational frequencies of the individual monomers. (The frequency shifts obtained from the MP2 and B3LYP theories are consistent with each other in direction and magnitude.) The stretching mode of the OH bond, whose predicted change in length as discussed earlier, produced the largest shift as the frequency is red-shifted by 561 cm^{-1}. The lower frequency of the OH stretching mode is consistent with the increased length of the bond. The larger bond length should also produce a greater intensity for the OH stretching mode, as the spin density surrounding the oxygen and hydrogen is spread further across the lengthened bond of the complex. This should also lead to an increase in the dipole moment. The calculations are in agreement with these predictions, and the intensity of the OH stretching mode is shown to increase by a factor of 10. The OH stretching mode of the complex is additionally expected to be the most intense band of the spectrum, also by a factor of 10. The dipole moment of the complex is 4.13 D, as compared to 2.64 D for the isolated radical. The increase in dipole moment is consistent with the increased intensity. The largest shift in terms of increasing frequency comes from the HOS bending mode, which is blue-shifted by 251 cm^{-1}. The HOS angle was free to bend in the radical monomer, but with the formation of the ring structure of the complex, the angle's movement is restricted, shortening any vibrational bending and thereby increasing the frequency at which the vibration occurs. The intensity of this mode in the complex is nearly doubled as compared to the intensity of the mode in the radical monomer. These two large shifts are similar to shifts reported in previous related work done by Aloisio and Francisco[29] regarding the HO_2-H_2O complex. In their study, the equivalent of the OH stretch of $HOSO_2$, the OH stretching mode of the hydroperoxy radical, underwent a large red shift and a 22-fold increase in intensity, and the comparable HOO bending mode of the same radical was blue-shifted by 120 cm^{-1} and the intensity is approximately doubled.[29] The analogous nature of frequency shifts in the two complexes shows the general effect of water on certain radicals, more specifically, radicals containing an available hydrogen and oxygen for bonding interactions with an oxygen and the hydrogen of water, respectively.

Similar hydrogen-bonding interactions have also been examined in closed shell−water complexes. The six-membered ring complex discussed here is very similar to the ring of the $H_2SO_4-H_2O$ complex, the product of water-catalyzed SO_3 conversion discussed previously.[22,25,39−41] Beichert and Schrems[39] examined the OH stretch of the participating hydroxyl group of H_2SO_4. The OH bond length increased by 0.030 Å in $HOSO_2-H_2O$ resulting in a −14.6% frequency shift. The same bond is increased by 0.026 Å in $H_2SO_4-H_2O$ and results in a −16.2% frequency shift.[39]

The electron spin densities of the isolated $HOSO_2$ radical and the complex are reported in Table 4. As shown, the sulfur atom of the system experiences an increase in spin density when the complex is formed. The increase of spin surrounding the lone sulfur atom conforms with the expected reduction and resulting increase in strength of the SO bond. It follows that the oxygen and hydrogen of the weakened OH bond of the complex should lose spin density as compared to the same atoms of the monomer, and a loss at both atoms is what is found. A spin density difference plot is presented in Figure 3. As the illustration shows, the spin density initially surrounding the OH bond of $HOSO_2$ has migrated in two directions, toward the sulfur atom and toward the oxygen of the water monomer. As expected, the figure shows no loss of spin density surrounding the sulfur. The density map clearly shows that the spin density surrounding the original monomers has reorganized in a ring fashion around the produced complex. An increase in spin density is clearly shown between the O′ of $HOSO_2$ and the H′ of H_2O. There is also a band of increased density on the backside of the structure surrounding the hydrogen of $HOSO_2$ and the oxygen of H_2O. The new spin densities found in these locations strongly support the existence of the bonding interactions

TABLE 3: Harmonic Vibrational Frequencies (cm^{-1}) and Intensities (km mol^{-1}) for $HOSO_2-H_2O$

			frequency (cm^{-1})[a]				intensity (km mol^{-1})			
			B3LYP		MP2		B3LYP		MP2	
species	mode number	mode description	6-31G(d)	6-311++ G(2df,2p)	6-31G(d)	6-311++ G(2df,2p)	6-31G(d)	6-311++ G(2df,2p)	6-31G(d)	6-311++ G(2df,2p)
	ν_1	OH stretch	3681	3753	3685	3776	105	134	131	152
	ν_2	O'SO″ asym stretch	1252	1290	1453	1419	104	156	465	294
	ν_3	HOS bend	1125	1112	1162	1163	87	72	143	111
	ν_4	O'SO″ sym stretch	1053	1084	1148	1131	57	78	51	69
$HOSO_2$	ν_5	SO stretch	725	735	780	790	139	161	170	183
	ν_6	OSO′ bend	502	520	542	552	35	27	45	33
	ν_7	O'SO″ bend	400	422	420	438	11	10	59	42
	ν_8	OSO'O″ torsion	390	414	415	435	35	34	16	17
	ν_9	HOSO′ torsion	248	285	285	317	104	87	98	79
H_2O	ν_1	H′O‴H″ asym stretch	3877	3923	4002	3995	13	62	29	78
	ν_2	H′O‴H″ sym stretch	3762	3820	3865	3871	0.14	8	0.62	11
	ν_3	H′O‴H″ bend	1708	1632	1738	1649	88	71	100	67
	ν_1	H′O‴H″ asym stretch	3808	3892 (−31)	3867	3946 (−49)	94	124	113	143
	ν_2	H′O‴H″ sym stretch	3664	3767 (−51)	3725	3802 (−69)	86	49	51	53
	ν_3	OH stretch	3036	3192 (−561)	3154	3223 (−553)	1199	1247	1157	1267
	ν_4	H′O‴H″ bend	1706	1627 (−5)	1727	1645 (−4)	76	80	79	66
	ν_5	HOS bend	1413	1362 (+251)	1460	1421 (+258)	93	114	310	257
	ν_6	O'SO″ asym stretch	1199	1237 (−52)	1348	1322 (−97)	110	138	208	127
	ν_7	O'SO″ sym stretch	1038	1072 (−12)	1141	1149 (+18)	76	94	103	117
	ν_8	OHO‴ bend	890	834	897	878	130	109	148	105
	ν_9	SO stretch	782	791 (+56)	844	851 (+61)	113	137	147	153
$HOSO_2-H_2O$	ν_{10}	O‴H′O′ bend	602	529	561	562	359	32	186	37
	ν_{11}	H′O‴H″ wag	510	480	551	496	29	107	188	117
	ν_{12}	O'SO″ bend	435	437	445	452	14	15	14	21
	ν_{13}	OSO″ bend	412	419	425	434	35	85	31	76
	ν_{14}	HO‴H′H″ torsion	344	311	331	315	43	82	61	82
	ν_{15}	HO‴H″H′ torsion	249	220	241	228	14	70	18	59
	ν_{16}	H′O‴H″H torsion	226	211	211	208	1	29	84	48
	ν_{17}	H′O′ stretch	162	109	151	129	5	18	15	15
	ν_{18}	OSO'O″ torsion	50	62	57	66	10	0.63	0.39	0

[a] Frequency shifts relative to monomers are given in parentheses.

TABLE 4: Electron Spin Densities[a] for $HOSO_2$ and $HOSO_2-H_2O$

	spin density			spin density	
atom	$HOSO_2$	$HOSO_2-H_2O$	atom	$HOSO_2$	$HOSO_2-H_2O$
S	0.5242	0.5587	O″	0.2052	0.2082
O	0.0855	0.0837	O‴		−0.0032
H	−0.0026	−0.0039	H′		−0.0005
O′	0.1877	0.1553	H″		0.0016

[a] MP2/6-311++G(3df,3pd) level of theory.

necessary for the formation of the two partial bonds used to hold the complex together. Morokuma energy decomposition analysis[42] of several radical−water complexes exhibiting the kind of double bonding found in $HOSO_2-H_2O$ has shown that these complexes result from electrostatic and exchange repulsion forces.[43] The calculated binding energies of the radical complex are given in Table 5. MP2 and B3LYP methods both give an uncorrected binding energy close to 15.5 kcal mol^{-1} using the 6-31G(d) basis set. With the next largest basis set, 6-311++G-(2d,2p), both calculations drop to 10.6 kcal mol^{-1}. Calculations at the following two basis sets provided a sequential increase in the binding energy for both levels of theory. The B3LYP method produced modest increases of 0.1−0.2 kcal mol^{-1} in energy from the 6-311++G(2d,2p) to 6-311++G(2df,2p) and then on to the 6-311++G(3df,3pd) basis set. The MP2 method calculated a large jump between 6-311++G(2d,2p) and 6-311++G(2df,2p) of nearly 2 kcal mol^{-1}. G2 and G3 calculations were also performed for the binding energy and produced results consistent with the MP2 results with the large basis sets. Table 5 shows that the binding energy calculated using B3LYP and MP2 methods converges as higher order valence electronic correlations and larger basis sets are used. The table also provides the G2 and G3 binding energies, which support the reliability of MP2. The D_e of 12.9 kcal mol^{-1} predicted from these calculations is the energy produced from the MP2 method using the 6-311++G(3df,3pd) basis set. Corrections for vibrational zero-point energy produce a D_o value of 10.6 kcal mol^{-1}, using the largest basis set. The nearly 11 kcal mol^{-1} corrected binding energy indicates that the complex should be experimentally observable and relatively stable under most atmospheric conditions. Table 6 reports the binding energy of four previously studied radical complexes[29,30,44−46] and the $HOSO_2-H_2O$ complex of this paper. In comparison to the other water complexes, $HOSO_2-H_2O$ is predicted to be the most tightly bound system of the group. The six-membered double hydrogen-bonded ring structure and essential preservation of the geometries for both monomers are possibilities for why the complex is so stable. At the MP2/6-311++G(2d,2p) level of theory, $HOSO_2-H_2O$ has a D_e of 10.7 kcal mol^{-1} and $H_2SO_4-H_2O$ has a D_e of 12.5 kcal mol^{-1}.[39]

The equilibrium constant for the complex produced in the reaction of the isolated monomers

$$HOSO_2 + H_2O \rightleftarrows HOSO_2-H_2O \qquad (9)$$

is derived from partition functions and statistical thermodynamics.[47] Data obtained via the ab initio calculations are used to determine the translational, vibrational, rotational, and electronic partition functions. More specifically, the binding energy calculated at the MP2/6-311++G(3df,3pd) level of theory and the rotational constants and vibrational frequencies calculated at the MP2/6-311++G(2df,2pd) level of theory are used in the partition function calculations. The total partition functions of

TABLE 5: Total and Binding Energies of $HOSO_2-H_2O$

		total energy (hartrees)			binding energy[a] (kcal mol^{-1})	
level of theory	basis set	$HOSO_2$	H_2O	$HOSO_2-H_2O$	D_e	D_o
B3LYP	6-31G(d)	−624.3532	−76.4090	−700.7873	15.7	13.5
	6-311++G(2d,2p)	−624.4972	−76.4620	−700.9762	10.6	8.4
	6-311++G(2df,2p)	−624.5173	−76.4626	−700.9971	10.7	8.5
	6-311++G(3df,3pd)	−624.5286	−76.4645	−701.0104	10.9	8.7
MP2	6-31G(d)	−623.2552	−76.1992	−699.4794	15.6	13.4
	6-311++G(2d,2p)	−623.6924	−76.3174	−700.0268	10.7	8.4
	6-311++G(2df,2p)	−623.7946	−76.3362	−700.1506	12.4	10.2
	6-311++G(3df,3pd)	−623.8567	−76.3477	−700.2249	12.9	10.6
G2		−623.6993	−76.3321	−700.0471		9.9
G3		−624.1569	−76.3820	−700.5552		10.2

[a] Single point calculated with the B3LYP/6-311++G(2df,2p) geometry.

Figure 3. Density difference plot of $HOSO_2-H_2O$.

TABLE 6: Comparison of Stability of Radical−Water Complexes

radical−water complex	D_e	D_o	ref
$HO-H_2O$[a]	5.6		44,45
HO_2-H_2O[b]	9.4	6.2	29
HO_3-H_2O[c]	7.0	4.9	46
$HOCO-H_2O$[d]	9.5	7.1	30
$HOSO_2-H_2O$[e]	10.9	8.6	this work

[a] Using RCISD(Q)/TZ2P. [b−e] Using B3LYP/6-311++G(3df,3pd).

the monomers and the complex are used to calculate the equilibrium constant as shown in the following equation:

$$K_{eq}(T) = \rho_{HOSO_2-H_2O}/\rho_{HOSO_2}\rho_{H_2O} \qquad (10)$$

where $K_{eq}(T)$ is the temperature-dependent equilibrium constant

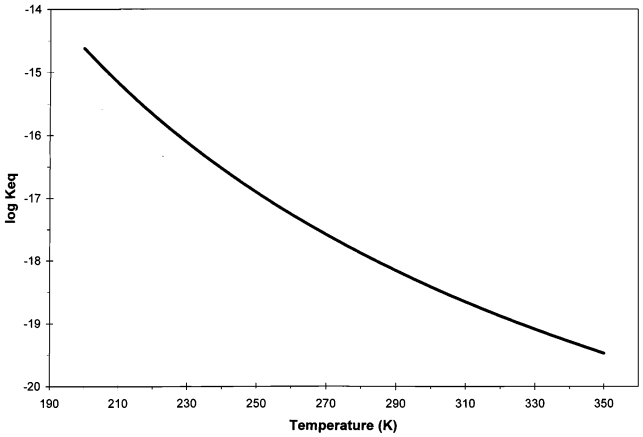

Figure 4. $HOSO_2-H_2O$ equilibrium constant as a function of temperature.

with units of cm^3 molecule^{-1} and $\rho_{HOSO_2-H_2O}$, ρ_{HOSO_2}, and ρ_{H_2O} are the total partition functions of the monomers and complex. Figure 4 indicates the calculated equilibrium constant from 200 to 350 K. For stratospherically relevant temperatures, K_{eq}^{210} is calculated as 6.8×10^{-16} cm^3 molecule^{-1} and K_{eq}^{270} equals 2.6×10^{-18} cm^3 molecule^{-1}. The formation of the complex is favored by nearly 300 times at 210 K than at 270 K. Using the determined equilibrium constants, the percentage of $HOSO_2$ that would complex with water can be estimated for different areas of the atmosphere. Lower temperatures and higher H_2O concentrations favor complex formation; therefore, the complex is more likely found in the lower regions of the stratosphere. At 30 km, the stratospheric concentration of H_2O is approximately 1.6×10^{12} molecules cm^{-3}, the temperature is 230 K,[48] and the corresponding equilibrium constant is 7.7×10^{-17} molecules cm^{-3}. Under these conditions, it is calculated that only 0.01% of available $HOSO_2$ radical would be complexed as $HOSO_2-H_2O$. At 10 km, the tropospheric concentration of H_2O is 2 orders of magnitude greater, the temperature is 220 K,[48] and the corresponding equilibrium constant is 2.2×10^{-16} cm^3 molecule^{-1}. The increase in H_2O concentration and the decrease in temperature result in increased conversion to roughly 2%. In the troposphere, temperature increases at lower altitudes, but water density levels continue to increase at a much faster rate than in the stratosphere. The greater concentration of water will dominate in the troposphere and be the driving force in complex formation. For example, a 300 K warm air mass at 80% humidity contains 7.8×10^{17} molecules cm^{-3} and the corresponding equilibrium constant is 9.6×10^{-19} cm^3 molecule^{-1}. Despite the warmer temperature, the large H_2O concentration would result in 25% conversion of $HOSO_2$ into the $HOSO_2-H_2O$ complex. With these conditions, complex formation could play an important role in the atmosphere. If

the complex was as strongly favored in regions of the troposphere, as suggested by the thermodynamic data, then a mechanism following the reaction 9 route for the formation of H_2SO_4 must be considered. In such a mechanism, reaction 2 would be replaced with a combination of reaction 9 and reaction 11.

$$HOSO_2-H_2O + O_2 \rightarrow SO_3-H_2O + HO_2 \qquad (11)$$

The next step of the mechanism would then involve the conversion of SO_3-H_2O to H_2SO_4. Morokuma and Muguruma[25] suggested in their study of the reaction of SO_3 with water that there are three possible reactions to convert SO_3 to H_2SO_4, either via reactions 6, 7, or 8. If reaction 11 was to produce a significant amount of SO_3-H_2O, it follows that reaction 7 seems to be the most plausible route to complete the mechanism.

If reaction 11 does indeed play a role in the lower atmosphere, it sheds new light on the reactions proposed by Morokuma and Muguruma,[25] suggesting that the final step of the H_2SO_4 mechanism would be completed by reaction 7 and not reactions 6 or 8. For reaction 11 to occur, however, the problems with the reaction must be considered. It is possible that a water complex may not have a catalytic effect but will instead slow the production of SO_3 in any form of a complex, because of the approach of the O_2 in extracting the hydrogen from the $HOSO_2$ in the complex. Of course, this would have to be balanced out by a weakened HO bond in $HOSO_2$ in the complex, which makes it easier for the hydrogen to be extracted once the O_2 is the best position. The formation of a $HOSO_2-H_2O$ complex may present alternate reaction pathways that do not follow the conventional mechanism for SO_3 conversion to H_2SO_4. Such alternate reaction pathways that might be possible through the use of the $HOSO_2-H_2O$ complex need to be examined in the future in hopes of fully understanding the role of water in all levels of the conversion of SO_2 to H_2SO_4.

IV. Conclusion

The structure and vibrational frequencies of the $HOSO_2-H_2O$ complex have been presented. The complex is suggested to exist as a six-membered ring structure exhibiting double hydrogen bonding. The $HOSO_2-H_2O$ complex is strongly bound by 10.6 kcal mol^{-1}.

References and Notes

(1) Acid Deposition. *Atmospheric Process in Eastern North America*; National Research Council, National Academy Press: Washington, DC, 1983.

(2) Calvert, J. G.; Lazrus, A.; Kok, G. L.; Heikes, B. G.; Walega, J. G.; Lind, J.; Cantrell, C. A. *Nature* **1985**, *317*, 27.

(3) Calvert, J. G.; Stockwell, W. R. In *SO2, NO and NO2 Oxidation Mechanisms: Atmospheric Considerations*; Acid Precipitation Series 3; Calvert, J. G., Teasely, J. I., Eds.; Butterworth Publishers: Boston, MA, 1984.

(4) Anderson, L. G.; Gates, P. M.; Nold, C. R. In *Biogenic Sulfur in the Environment*; Saltzman, E. S., Cooper, W. J., Eds.; American Chemical Society: Washington, DC, 1989.

(5) Calvert, J. G.; Su, Fu; Bottenheim, J. W.; Strauz, O. P. *Atmos. Environ.* **1978**, *19*, 1029.

(6) Martigan, J. J. *J. Phys. Chem.* **1984**, *88*, 3314.

(7) Wine, P. H.; Thompson, R. J.; Ravishankara, A. R.; Semmes, D. H.; Gump, C. A.; Torabi, A.; Nicovich, J. M. *J. Phys. Chem.* **1984**, *88*, 2095.

(8) Egsgaard, H.; Carlsen, L.; Florencio, H.; Drewello, T.; Schwarz, H. *Chem. Phys. Lett.* **1988**, *148*, 537.

(9) Greenblatt, G. D.; Howared, C. J. *J. Phys. Chem.* **1989**, *93*, 1035.

(10) Lee, Y. Y.; Kao, W. C.; Lee, Y. P. *J. Phys. Chem.* **1990**, *94*, 4535.

(11) Martin, D.; Jourdain, J. L.; Bras, G. L. *J. Phys. Chem.* **1986**, *90*, 4143.

(12) Nagase, S.; Hasimoto, S.; Akimoto, H. *J. Phys. Chem.* **1988**, *92*, 641.

(13) Stockwell, W. R.; Calvert, J. G. *Atmos. Environ.* **1983**, *17*, 2231.

(14) Hashimoto, S.; Inoue, G.; Akimoto, H. *Chem. Phys. Lett.* **1984**, *107*, 198.

(15) Majumdar, D.; Kim, G.; Kim, J.; Oh, K. S.; Lee, J. Y.; Kim, K. S.; Choi, W. Y.; Lee, S.; Kang, M.; Mhin, B. J. *J. Chem. Phys.* **2000**, *112*, 723.

(16) Gleason, J. F.; Sinha, A.; Howard, C. J. *J. Phys. Chem.* **1987**, *91*, 719.

(17) Wang, X.; Jin, Y. G.; Suto, M.; Lee, L. C.; O'Neal, H. E. *J. Chem. Phys.* **1988**, *89*, 4853.

(18) Polevoi, P S.; Khachaturov-Tavrizian, A. E.; Ivanov, I. N. *Radiat. Phys. Chem.* **1990**, *36*, 99.

(19) Reiner, T.; Arnold, F. *J. Chem. Phys.* **1994**, *101*, 7399.

(20) Lovejoy, E. R.; Hanson, D. R.; Huey, L. G. *J. Phys. Chem.* **1996**, *100*, 19911.

(21) Brown, R. C.; Anderson, M. R.; Miake-Lye, R. C.; Kolb, C. E.; Sorokin, A. A.; Buriko, Y. Y. *Geophys. Res. Lett.* **1996**, *23*, 3603.

(22) Kolb, C. E.; Jayne, J. T.; Worsnop, D. R.; Molina, M. J.; Meads, R. J.; Viggiano, A. A. *J. Am. Chem. Soc.* **1994**, *116*, 10314.

(23) Chen, T. S.; Plummer, P. L. M. *J. Phys. Chem.* **1985**, *89*, 3689.

(24) Hofmann, M.; Schleyer, P. v. R. *J. Am. Chem. Soc.* **1994**, *116*, 4947.

(25) Morokuma, K.; Muguruma, C. *J. Am. Chem. Soc.* **1994**, *116*, 10316.

(26) Hofmann-Sievert, R.; Castleman, A. W. *J. Phys. Chem.* **1984**, *88*, 3329.

(27) Akhmatskaya, E. V.; Apps, C. J.; Hillier, I. H.; Masters, A. J.; Wat, N. E.; Whitehead, J. C. *Chem. Commun.* **1997**, 707.

(28) Li, W.; McKee, M. L. *J. Phys. Chem. A* **1997**, *101*, 9778.

(29) Aloisio, S.; Francisco, J. S. *J. Phys. Chem. A* **1998**, *102*, 1899.

(30) Aloisio, S.; Francisco, J. S. *J. Phys. Chem. A* **2000**, *104*, 404.

(31) Frisch, M. J.; Trucks, G. W.; Schlegel, H. B.; Scuseria, G. E.; Robb, M. A.; Cheeseman, J. R.; Zakrzewski, V. G.; Montgomery, J. A., Jr.; Stratmann, R. E.; Burant, J. C.; Dapprich, S.; Millam, J. M.; Daniels, A. D.; Kudin, K. N.; Strain, M. C.; Farkas, O.; Tomasi, J.; Barone, V.; Cossi, M.; Cammi, R.; Mennucci, B.; Pomelli, C.; Adamo, C.; Clifford, S.; Ochterski, J.; Petersson, G. A.; Ayala, P. Y.; Cui, Q.; Morokuma, K.; Malick, D. K.; Rabuck, A. D.; Raghavachari, K.; Foresman, J. B.; Cioslowski, J.; Ortiz, J. V.; Stefanov, B. B.; Liu, G.; Liashenko, A.; Piskorz, P.; Komaromi, I.; Gomperts, R.; Martin, R. L.; Fox, D. J.; Keith, T.; Al-Laham, M. A.; Peng, C. Y.; Nanayakkara, A.; Gonzalez, C.; Challacombe, M.; Gill, P. M. W.; Johnson, B. G.; Chen, W.; Wong, M. W.; Andres, J. L.; Head-Gordon, M.; Replogle, E. S.; Pople, J. A. *Gaussian 98*, revision A.7; Gaussian, Inc.: Pittsburgh, PA, 1998.

(32) Møller, C.; Plesset, M. S. *Phys. Rev. B* **1934**, *46*, 618.

(33) Frisch, M. J.; Head-Gordon, M.; Pople, J. A. *J. Chem. Phys.* **1990**, *141*, 189.

(34) Becke, A. D. *J. Chem. Phys.* **1993**, *98*, 5648.

(35) Lee, C.; Yang, W.; Parr, R. G. *Phys. Rev. B* **1988**, *37*, 785.

(36) Ditchfield, R.; Hehre, W. J.; Pople, J. A. *J. Chem. Phys.* **1971**, *54*, 724.

(37) Frisch, M. J.; Pople, J. A.; Binkley, J. S. *J. Chem. Phys.* **1984**, *80*, 3265.

(38) Boys, S. F.; Bernardi, F. *Mol. Phys.* **1970**, *19*, 533.

(39) Beichert, P.; Schrems, O. *J. Phys. Chem. A* **1998**, *102*, 10540.

(40) Arstila, H.; Laasonen, K.; Laaksonen, A. *J. Chem. Phys.* **1998**, *108*, 1031.

(41) Bandy, A. R.; Ianni, J. C. *J. Phys. Chem. A* **1998**, *102*, 6533.

(42) Morokuma, K. *J. Chem. Phys.* **1971**, *55*, 1236.

(43) Gora, R. W.; Roszak, S.; Francisco, J. S. Unpublished result.

(44) Kim, K. S.; Kim, H. S.; Jung, J. H.; Mhin, B. J.; Xie, Y.; Schaefer, H. F., III. *J. Chem. Phys.* **1991**, *94*, 2057.

(45) Xie, Y.; Shaefer, H. F., III. *J. Chem. Phys.* **1993**, *98*, 8829.

(46) Aloisio, S.; Francisco, J. S. *J. Am. Chem. Soc.* **1999**, *121*, 8592.

(47) McQuarrie, D. A. *Statistical Thermodynamics*; Harper and Row: New York, 1973.

(48) DeMore, W. B.; Sander, S. P.; Golden, D. M.; Hampson, R. F.; Kurylo, M. J.; Howard, C. J.; Ravishankara, A. R.; Kolb, C. E.; Molina, M. J. *Chemical Kinetics and Photochemical Data for Use in Stratospheric Modelling*; Evaluation No. 12; National Aeronautics and Space Administration−Jet Propulsion Laboratory: Pasadena, 1997.